



## Research article

# A novel self-enhanced electrochemiluminescent aptamer sensor based on ternary nanocomposite PEI/RuSi-MWCNTs for the detection of profenofos residues in vegetables

Zhenying He<sup>a,b,c,d</sup>, Haifang Wang<sup>e</sup>, Wenzheng Liu<sup>a,c,d</sup>, Jiashuai Sun<sup>a,c,d</sup>,  
Jingcheng Huang<sup>a,c,d</sup>, Jie Han<sup>a,c,d</sup>, Baoxin Li<sup>a,c,d</sup>, Rui Xu<sup>a,c,d</sup>, Yuhao Zhang<sup>a,c,d</sup>,  
Jin Hua<sup>a,c,d</sup>, Yemin Guo<sup>a,c,d</sup>, Fangyuan Lu<sup>a,c,d,\*</sup>, Ce Shi<sup>b,\*\*</sup>

<sup>a</sup> School of Agricultural Engineering and Food Science, Shandong University of Technology, No. 266 Xincun Xilu, Zibo, Shandong, 255049, China

<sup>b</sup> Information Technology Research Center, Beijing Academy of Agriculture and Forestry Sciences, Beijing, 100097, China

<sup>c</sup> Zibo City Key Laboratory of Agricultural Product Safety Traceability, No. 266 Xincun Xilu, Zibo, Shandong, 255049, China

<sup>d</sup> Shandong Provincial Engineering Research Center of Vegetable Safety and Quality Traceability, No. 266 Xincun Xilu, Zibo, Shandong, 255049, China

<sup>e</sup> Dongzhimen Hospital, Beijing University of Chinese Medicine, Beijing, 100700, China

## ARTICLE INFO

## Keywords:

Electrochemiluminescence  
Ru(bpy)<sub>3</sub><sup>2+</sup>  
Multi-walled carbon nanotubes  
Profenofos  
Aptasensor

## ABSTRACT

In this work, a novel ternary nanocomposite of PEI/RuSi-MWCNTs was designed and synthesized for the first time, which an ultrasensitive and self-enhanced electrochemiluminescent (ECL) aptasensor was developed for the detection of profenofos residues in vegetables. The self-enhanced complex PEI-Ru (II) enhanced the emission and stability of ECL, and the multi-walled carbon nanotubes (MWCNTs) acted as an excellent carrier and signal amplification. The PEI/RuSi-MWCNTs were characterized by scanning electron microscope (SEM), transmission electron microscope (TEM) and energy dispersive spectrometer (EDS). The incorporation of gold nanoparticles (AuNPs) improved the performance of the sensor and provided a platform for the immobilization of the aptamer. The results of the experiment showed that the presence of profenofos significantly suppressed the electrochemiluminescence intensity of the sensor. The detection sensitivity of the aptamer sensor was in the range of  $1 \times 10^{-2}$  to  $1 \times 10^3$  ng/mL. Under optimal conditions, the limit of detection (LOD) of the sensor for profenofos was  $1.482 \times 10^{-3}$  ng/mL. The sensor had excellent stability, reproducibility and specificity. The recoveries of the sensor ranged from 92.29 % to 106.47 % in real sample tests.

## 1. Introduction

Organophosphorus pesticides (OPs) are extensively utilized in managing pests and diseases in vegetables, fruit trees and other crops. Because of their powerful insecticidal ability and low price, OPs account for about 34 % of pesticide production and sales [1],

\* Corresponding author. School of Agricultural Engineering and Food Science, Shandong University of Technology, No. 266 Xincun Xilu, Zibo, Shandong, 255049, China.

\*\* Corresponding author. Information Technology Research Center, Beijing Academy of Agriculture and Forestry Sciences, Beijing, 100097, China.  
E-mail addresses: [fangyuan-lu@foxmail.com](mailto:fangyuan-lu@foxmail.com) (F. Lu), [shice001@163.com](mailto:shice001@163.com) (C. Shi).

<https://doi.org/10.1016/j.heliyon.2024.e25167>

Received 15 November 2023; Received in revised form 20 January 2024; Accepted 22 January 2024

Available online 26 January 2024

2405-8440/© 2024 The Authors. Published by Elsevier Ltd. This is an open access article under the CC BY-NC-ND license (<http://creativecommons.org/licenses/by-nc-nd/4.0/>).

and are currently effective pesticides. OPs contain nerve agents [2], long-term unregulated use and misuse of OPs can result in serious residues. OPs can be harmful to the human nervous system because they inhibit the catalytic action of acetylcholinesterase in the human body [3], thereby increasing the risk of neurological diseases such as Parkinson's and Alzheimer's [4]. Data from World Health Organization (WHO) suggest that about 3,000,000 people are poisoned by OPs every year, and the number of deaths exceeds 300,000 [5]. As one of organophosphorus pesticides, profenofos is frequently employed in vegetables. Profenofos residues can harm human health through the consumption of fruits, vegetables and other foods [6] that accumulate in the body over time. Therefore, there arises a need for the rapid and precise detection of profenofos [7].

In recent years, there have been many mature pesticide residues detection methods, including liquid chromatography (LC) [8], gas chromatography (GC) [9], mass spectrometry (MS) [10,11]. These methods are accurate in test results. And the disadvantages are long detection time, high cost of detection, and the need for professional operators [12]. Electrochemical sensor and electrochemiluminescent sensor are being used more and more widely in the field of pesticide residues detection [13]. Zhao et al. developed a plant-wearable biosensor that enabled non-destructive and in situ analysis of pesticides on the surface of agricultural products [14]. Electrochemiluminescence (ECL) is a detection method that combines electrochemistry and chemiluminescence [15]. ECL characterized by its low limit of detection and extensive linear detection range, as a prominent research focus in the realm of biochemical analysis, because of its simple operation method, rapid detection reaction and easy miniaturization [16,17].

Aptamer (Apt) is an oligonucleotide fragment that is selected by systematic evolution of ligands by exponential enrichment (SELEX) screening for ligand phylogeny [18]. Due to its special spatial structure, it can specifically recognize target molecules. Aptamer is an ideal recognition element with wide target molecules, high affinity, high specificity and easy modification [19]. Aptamer is widely used in fluorescent sensors [20], electrochemical sensors and electrochemiluminescent sensors [21,22].

Tris (2,2'-bipyridyl) ruthenium (II) ( $\text{Ru}(\text{bpy})_3^{2+}$ ) serves as conventional luminophore for ECL detection and has found extensive utilization in electrochemiluminescent sensors due to its high emissivity and favorable electrochemical stability [23,24]. In electrochemiluminescence systems, the immobilization of luminophore to achieve an enhanced background response is an important element. Individual  $\text{Ru}(\text{bpy})_3^{2+}$  is difficult to be immobilized on the electrode surface. In this work, aminated  $\text{RuSiNPs}$  are synthesized by wrapping the luminophore  $\text{Ru}(\text{bpy})_3^{2+}$  with silica spheres, which possesses good stability and compatibility, and the attached amines are able to composite the luminophore better with the nanomaterial [25,26].

Intramolecular self-enhanced ECL refers to the co-embedding of luminescent substances and co-reactants in the same structure to shorten the electron transfer distance, thus improving the intensity and stability of luminescence [27]. In this work, polyethyleneimine (PEI) with amino groups was chosen not only as an ideal co-reactant for  $\text{Ru}(\text{bpy})_3^{2+}$  to enhance the strength of ECL, but also as an immobilization matrix for  $\text{RuSiNPs}$  to immobilize on carboxylated MWCNTs. Cao et al. established a novel self-enhanced ECL sensor, based on PEI-CdS/Au@SiO<sub>2</sub>/RuDS/PANI and creatinine imprinted poly (*ortho*-aminophenol) film [28]. Yuan et al. constructed a sensitive ECL immunosensor for carcinoembryonic antigen (CEA) detection by using the signal amplification effect of pL-Cys toward the self-enhanced PEI-Ru(II) complex [29]. It has been shown that it is feasible to enhance the ECL properties by immobilizing the self-enhanced ECL complex Ru-PEI onto various nanomaterials and thereby enhancing the ECL properties.

Carbon nanotubes (CNTs) are materials possessing sizable specific surface area and exceptional electron transfer capability [30]. With the maturation of nanotechnology, multi-walled carbon nanotubes (MWCNTs) are widely used for signal amplification in sensors [31]. MWCNTs are carbon materials with excellent conductivity and special spatial structure [32], and are increasingly used by researchers to make substrate materials for biosensors. MWCNTs have poor water solubility and agglomerate in water, while the excellent water solubility of PEI allows MWCNTs to be dispersed in solution [33]. Due to the good plasmon resonance effect [34], gold nanoparticles (AuNPs) are often employed to enhance electron conductivity [35]. The introduction of AuNPs in the sensor can improve the electron transfer capability of the sensor, while AuNPs can also immobilize the aptamer through gold-sulfur (Au-S) bonds [36].

In this paper, PEI/ $\text{RuSi}$ -MWCNTs nanocomposites with self-enhanced structure were synthesized for the first time by using PEI as a co-reactant of  $\text{Ru}(\text{bpy})_3^{2+}$ . PEI effectively improves the luminescence efficiency of  $\text{RuSiNPs}$  [37]. The carboxylated MWCNTs can immobilize the  $\text{RuSiNPs}$  with amino groups and PEI on the surface through amide reaction [38], and at the same time they play the role of signal amplification. The composite of PEI/ $\text{RuSi}$ -MWCNTs has a self-enhanced structure, which shortens the electron transfer distance, reduces the energy loss due to the long path and improves the ECL strength [39]. In this experiment, we immobilized PEI/ $\text{RuSi}$ -MWCNTs as substrates on the surface of a glassy carbon electrode (GCE). The addition of AuNPs was used to immobilize the sulfhydryl-modified aptamer and enhance the redox response of ECL. We used the aptamer of profenofos as the recognition material. The ECL aptasensor prepared in this work has good stability, specificity and remarkable sensitivity, which provides a solution to detect profenofos residues in vegetables.

## 2. Experimental

### 2.1. Material

Tris (2,2'-bipyridyl) ruthenium (II) chloride hexahydrate and Gold (III) chloride trihydrate ( $\text{HAuCl}_4 \cdot 3\text{H}_2\text{O}$ ) were purchased from Shanghai Macklin Biochemical Co., Ltd. (Shanghai, China). MWCNTs (>95 % purity), polyethyleneimine, 1-Hexanol, cyclohexane,  $\text{NH}_4\text{OH}$ , anhydrous ethanol, acetone, KCl, NaCl,  $\text{NaH}_2\text{PO}_4 \cdot 2\text{H}_2\text{O}$ ,  $\text{Na}_2\text{HPO}_4 \cdot 12\text{H}_2\text{O}$ , trisodium citrate dihydrate, potassium ferricyanide were purchased from Sinopharm Chemical Reagent Co., Ltd. (Shanghai, China). Profenofos, malathion, chlorpyrifos and acetamiprid were purchased from Beijing Putian Tongchuang Biotechnology Co., Ltd. (Beijing, China).

The aptamer sequence selected with reference to this document was modified with sulfhydryl [40]. The sequence of aptamer was 5-(SH)-(CH<sub>2</sub>)<sub>6</sub>-AAGCTTTTTTACTGCAGGTGAAAAAGAG-3'. Aptamer, 1 × TE buff and bovine serum albumin (BSA) were purchased

from Sangon Biotech Co., Ltd. (Shanghai, China).

## 2.2. Apparatus

The electrochemical workstation (CHI-660D) was manufactured by Shanghai Chenhua Instrument Co., Ltd. (Shanghai, China). The electrochemiluminescence system (MPI-A) and its accessories were manufactured by Xian Remex Analysis Instrument Co., Ltd. (Xi'an, China). Ultrasonic cleaning instrument was produced by Shanghai Kedao Ultrasonic Instrument Co., Ltd. (Shanghai, China). Digital thermostatic magnetic stirrer and electronic analytical balance were produced from Mettler-Toledo Instruments (Shanghai) Co., Ltd. (Shanghai, China). High-speed benchtop centrifuge (Sorvall ST 16 R) was produced by Thermo Fisher Scientific (China) Co., Ltd. The pH meter (FE-20 K) was produced by Mettler-Toledo Instruments (Shanghai) Co., Ltd. (Shanghai, China). Ultra-pure water purification system was provided by the Milli-Q water purification system.

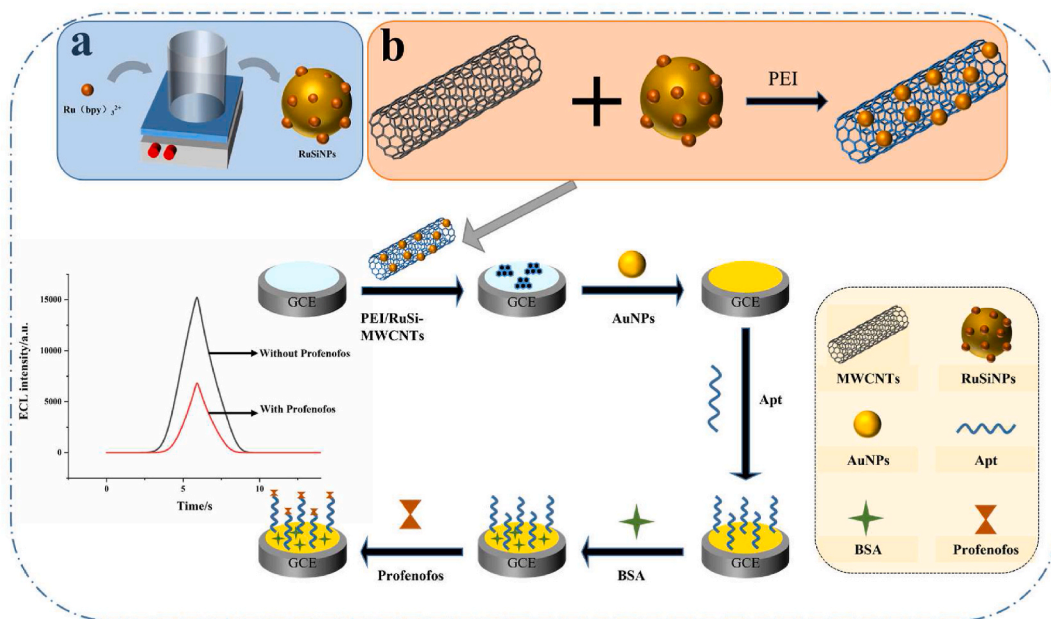
## 2.3. Preparation of PEI/RuSi-MWCNTs

RuSiNPs were prepared by reference to the reported W/O microemulsion method [41]. Microemulsions were created through the combination of 1.8 mL 1-hexanol, 1.77 mL Triton X-100, 7.5 mL cyclohexane, and 340  $\mu\text{L}$  40 mM  $\text{Ru}(\text{bpy})_3^{2+}$  under continuous magnetic stirring for 10 min. Subsequently, 200  $\mu\text{L}$  TEOS, 80  $\mu\text{L}$   $\text{NH}_4\text{OH}$  were added to the mixture and mixed and stirred for 20 h to obtain RuSiNPs. 10  $\mu\text{L}$  APTES was added, and stirring was continued for 4 h, and then acetone was added to disrupt the emulsion. The mixture underwent three rounds of washing via centrifugation using ethanol and water, respectively, to obtain the final orange  $\text{NH}_2$ -RuSiNPs. The  $\text{NH}_2$ -RuSiNPs were dispersed in PBS solution (pH 7.4, 0.1 M) for subsequent application.

5 mg carboxylated MWCNTs were dispersed into  $\text{H}_2\text{O}$  (10 mL), 40 mg EDC and 20 mg NHS were added. The mixture was sonicated for 30 min for activation of the carboxyl groups. Subsequently, 0.0125 g PEI and 3 mL  $\text{NH}_2$ -RuSiNPs were introduced into the activated MWCNTs solution, and the mixture was stirred at room temperature for 12 h. The reactants were subjected to centrifugation (8000 rpm, 15 min) to acquire PEI/RuSi-MWCNTs nanocomposites, which were finally dispersed into 10 mL PBS (pH 7.4, 0.1 M) and stored at 4  $^\circ\text{C}$  for further use. At this point, stop heating and continue stirring for 30 min to obtain PEI/RuSi-MWCNTs. Store the prepared PEI/RuSi-MWCNTs solution away from light at 4  $^\circ\text{C}$ . The synthesis of RuSi-MWCNTs was also carried out by taking the same material without adding PEI in the same experimental conditions.

## 2.4. Preparation of AuNPs

Refer to the previous method to prepare AuNPs [42]. The glassware utilized in the experiment was soaked in aqua regia for over 12 h, subsequently rinsed with ultrapure water, and then dried. First, 50 mL 0.01 %  $\text{HAuCl}_4 \cdot 3\text{H}_2\text{O}$  was boiled with stirring for 7–8 min, and rapidly added 1.0 mL aqueous trisodium citrate solution (1 %). Solution color changed gradually from light blue to become dark red. At this point, stop heating and continue stirring for 30 min to obtain AuNPs. Store the prepared AuNPs solution away from light at



**Scheme 1.** Schematic representation of the assembly procedure for the aptasensor: (a) Synthesis of RuSiNPs; (b) Formation process of PEI/RuSi-MWCNTs.

4 °C.

### 2.5. Fabrication of the aptasensor

Initially, the glassy carbon electrode (GCE) underwent polishing, involving the use of 0.3 mm  $\text{Al}_2\text{O}_3$  powder for the polishing process and then cleaned by ultrasonic cleaning for 30 s using a mixture of ethanol and ultrapure water. It was dried at room temperature with nitrogen gas and set aside.

Firstly, 5  $\mu\text{L}$  PEI/RuSi-MWCNTs was dripping onto the surface of the GCE and subsequently left to air-dry at room temperature. Then 5  $\mu\text{L}$  AuNPs were dropped on the PEI/RuSi-MWCNTs/GCE surface and allowed to air-dry naturally. 3  $\mu\text{L}$  sulfhydryl modified aptamer solution was added to the electrode surface and allowed to react for 1 h. The sulfhydryl groups of the aptamer and AuNPs formed gold-sulfur bonds, and the aptamer was immobilized on the electrode surface. The electrode surface was coated with 0.05 % BSA and reacted for 40 min to close the non-specific binding site. The unbound material was softly washed with ultrapure water. To validate the sensor's performance, 3  $\mu\text{L}$  profenofos was dripped onto the modified electrode to assess luminescence. The preparation step for preparing the ECL sensor and its underlying detection principle were depicted in [Scheme 1](#).

### 2.6. Sample pretreatment

The samples tested in this work were rape, spinach and lettuce, all of which were sourced from Zibo supermarkets. Through high-performance liquid chromatography (HPLC), it was determined that all samples exhibited no traces of profenofos residues.

Firstly, wash the vegetables with ultra-pure water and dry them naturally. The vegetables were cut into 1–2 mm pieces with a knife, 2 g vegetable samples were weighed and added to the centrifuge tube together with 3 mL different concentrations of profenofos, mixed and stirred, and left at room temperature for 16 h. As to the treatment of the mixture, 2 mL acetone and 18 mL 0.1 M PBS (pH 7.4, 0.1 M) were introduced and left for 2 h. The resulting samples were subjected to centrifugation (10,000 rpm, 10 min), and the supernatant was extracted for the subsequent assay.

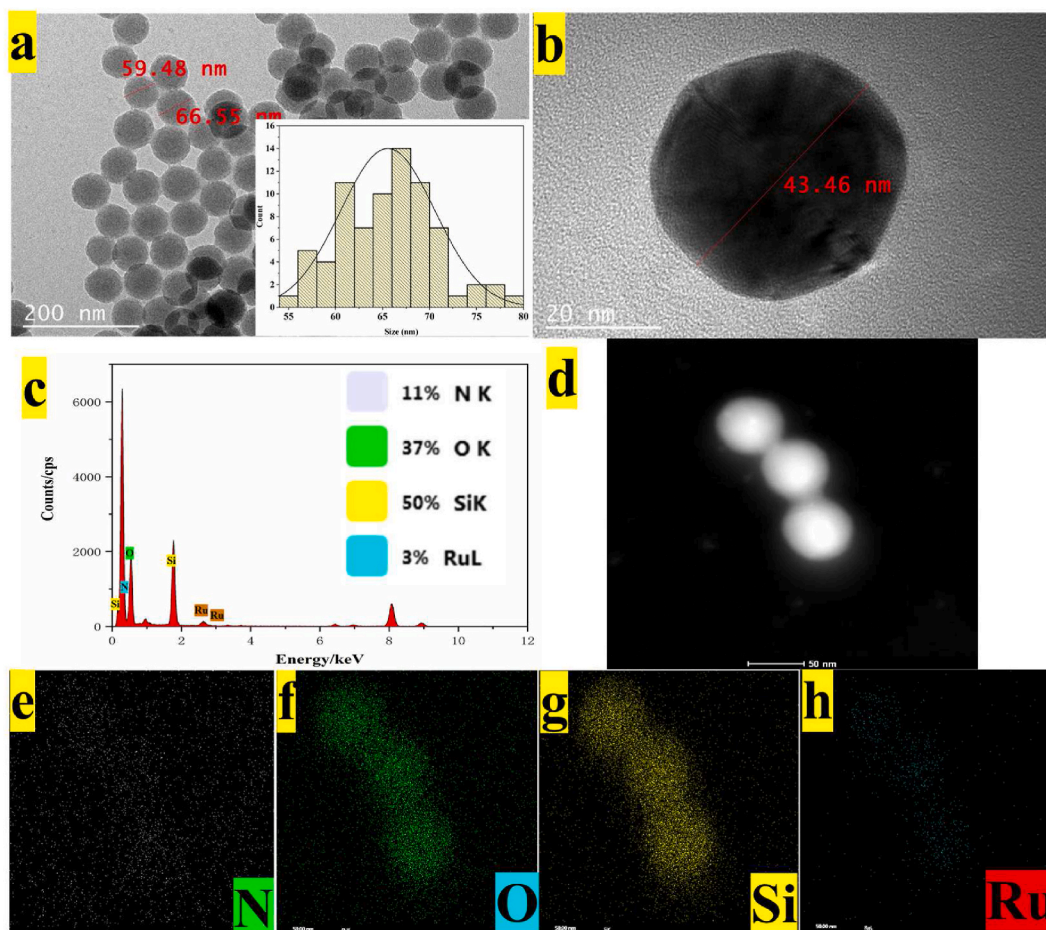


**Fig. 1.** TEM image of RuSiNPs (a, b); EDS spectrum of RuSiNPs (c); STEM-EDS mapping image of RuSiNPs (e–h).

### 3. Results and discussion

#### 3.1. Characterizations of nanomaterials

##### 3.1.1. RuSiNPs

Fig. 1. (a) and (b) showed the TEM images of RuSiNPs. The depicted image distinctly illustrated that the RuSiNPs synthesized by the water-in-oil microemulsion method was a sphere of about 50 nm in diameter. Fig. 1. (c) Showed the energy dispersive spectrometer (EDS) spectrum of RuSiNPs, from which it could be seen that RuSiNPs contained both N, O, Si and Ru. The presence of O, Si, and Ru elements indicated that Ru(bpy)<sub>3</sub><sup>2+</sup> was effectively synthesized with SiO<sub>2</sub>. The presence of N elements indicated that RuSiNPs were successfully aminated. As observed in Fig. 1 (d-h), Ru(bpy)<sub>3</sub><sup>2+</sup> and SiO<sub>2</sub> were doped structures.

##### 3.1.2. PEI/RuSi-MWCNTs

Fig. 2. (a) and Fig. 2. (b) illustrated the TEM images and SEM images of PEI/RuSi-MWCNTs, respectively. From the images, it could be seen that the fine rod-shaped MWCNTs, the spherical RuSiNPs and the lamellar PEI were combined together in a certain spatial structure. This was because the carboxyl groups of carboxylated MWCNTs and the amino groups of NH<sub>2</sub>-RuSiNPs and PEI were linked together by amide bonds. Fig. 2 (c, e-h) showed the EDS spectrum of PEI/RuSi-MWCNTs. The elemental distribution of C, N, Si, and Ru in the EDS spectrum of PEI/RuSi-MWCNTs in Fig. 2. (d) also proved the success of the material synthesis.

#### 3.2. ECL and electrochemical behavior of aptasensor

The ECL intensity of the layer-by-layer modified sensors was analyzed in the experiments. As shown in Fig. 3 (A), curve a showed the GCE with PEI/RuSi-MWCNTs added dropwise, it could be seen that the electrode with added nanocomposite had good ECL intensity, indicating that the composite had good ECL performance. Curve b showed AuNPs/PEI/RuSi-MWCNTs/GCE with the addition of AuNPs slightly enhancing the ECL strength. Upon immobilizing the aptamer onto the sensor via the Au-S bond, the addition of BSA

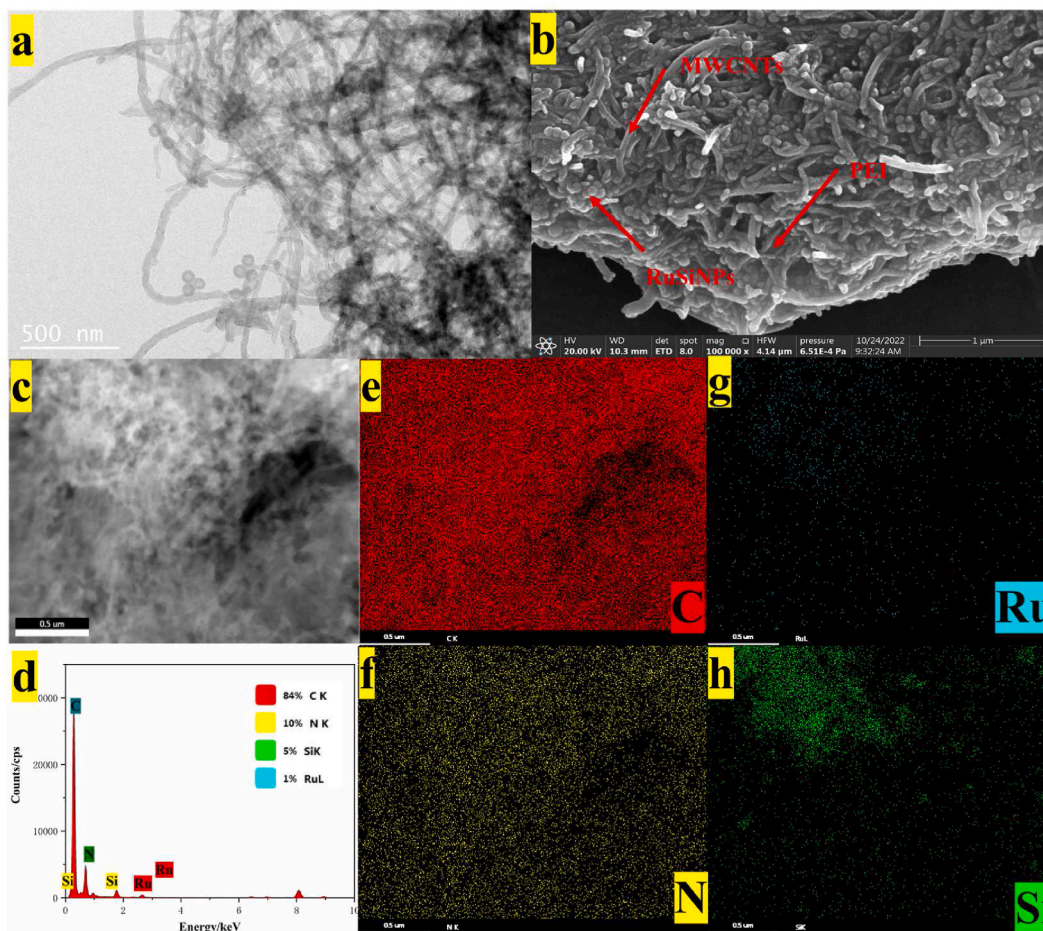
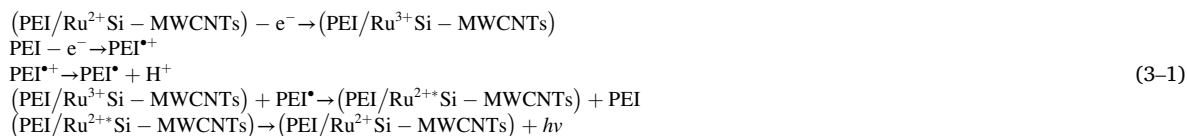


Fig. 2. TEM image of PEI/RuSi-MWCNTs (a); SEM image of PEI/RuSi-MWCNTs (b); EDS spectrum of PEI/RuSi-MWCNTs (c-h).

led to a noteworthy reduction in the ECL intensity of the sensor. This phenomenon was attributed to the creation of spatial barriers within the organic molecules, resulting in decreased electron transfer capacity and subsequently diminishing ECL intensity. Finally, the addition of profenofos caused a change in ECL intensity. Overall, these results further demonstrated the success of the sensor preparation.

In order to investigate the bursting mechanism, the luminescence intensity of the two composites, PEI/RuSi-MWCNTs and RuSi-MWCNTs, was compared. The luminescence intensity of the nanocomposites with added PEI was greatly enhanced as shown by curve a and curve g in Fig. 3A. It was proved that PEI could act as a co-reactant to amplify the signal of RuSiNPs. It was consistent with the previous report [43]. We speculated that the possible emission mechanism was inferred as follows:



As expressed in Eqs. (3)–(1),  $\text{Ru}^{2+}$  on the working electrode lost an electron to become  $\text{Ru}^{3+}$  under the action of the excitation voltage. At the same time, the PEI on the surface of the electrode became free radical  $\text{PEI}^{\bullet}$ . The strongly oxidising  $\text{Ru}^{3+}$  underwent a redox reaction with the free radical  $\text{PEI}^{\bullet}$ .  $\text{Ru}^{3+}$  was reduced to the excited state  $\text{Ru}^{2+*}$ . The excited state  $\text{Ru}^{2+*}$  decayed by releasing a photon which released energy and thus converted to the ground state  $\text{Ru}^{2+}$ . This completed the electrochemical luminescence process.

Fig. 3 (B) Showed the cyclic voltammetry (CV) characteristics of the aptasensor. The bare electrode exhibited a pair of reversible redox peaks (curve f). After the addition of PEI/RuSi-MWCNTs to the GCE surface, a notable enhancement in the sensor's current response was observed (curve a). This increase could be attributed to the exceptional conductivity of MWCNTs. There was a slight increase in current after the dropwise addition of AuNPs (curve b), which slightly enhanced the redox response at the sensor interface. After aptamer being bound, there was a clear decrease in the current response because the electrostatic repulsion between the aptamers reduced the electron transfer capacity of the electrode surface (curve c). The addition of BSA blocked the non-specific interactions on the electrode surface, resulting in a further reduction in peak current (curve d). Finally, the addition of profenofos, which bound specifically to the aptamer to form a complex, further reduced the conductivity of the sensor and the peak current decreased again

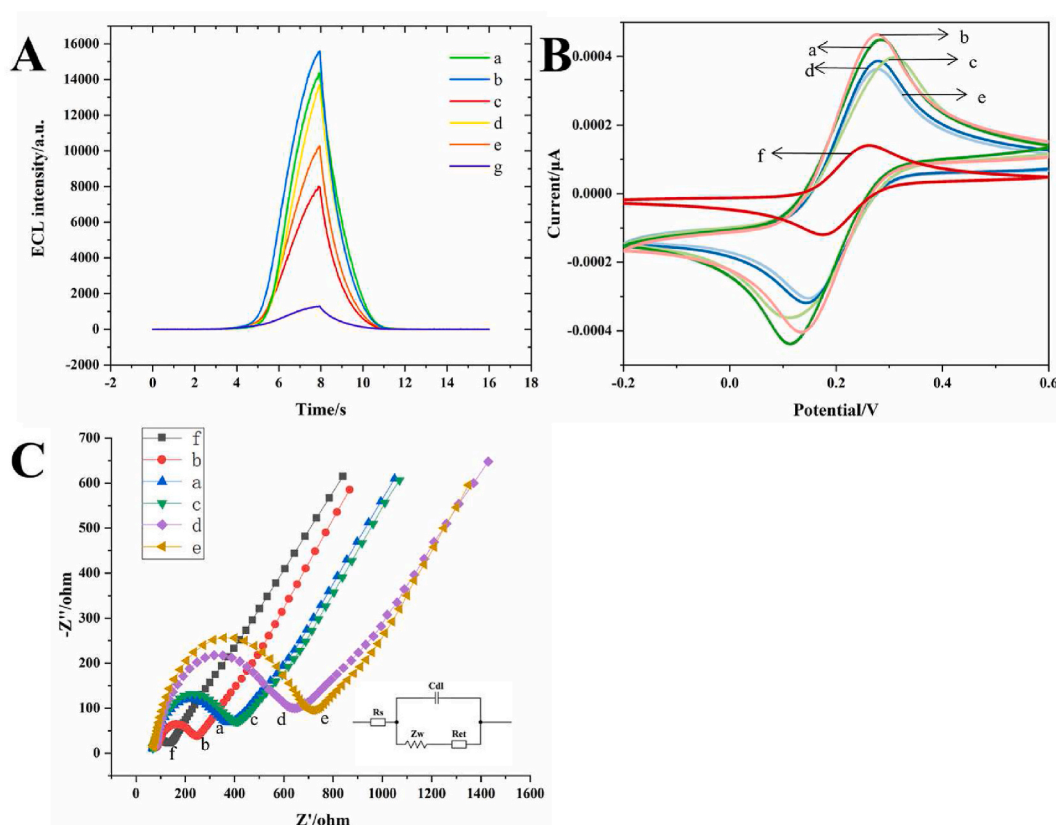


**Fig. 3.** (A) ECL intensity of material; (B) CV characterization of aptasensor assembly diagram; (C) EIS characterization of aptasensor assembly diagram: (a) PEI/RuSi-MWCNTs/GCE, (b) AuNPs/PEI/RuSi-MWCNTs/GCE, (c) apt/AuNPs/PEI/RuSi-MWCNTs/GCE, (d) BSA/apt/AuNPs/PEI/RuSi-MWCNTs/GCE, (e) Profenofos/BSA/apt/AuNPs/PEI/RuSi-MWCNTs/GCE, (f) bare GCE, (g) RuSi-MWCNTs/GCE.

(curve e).

Fig. 3 (C) Showed the electrochemical impedance spectroscopy (EIS) image characterization curve for the layer-by-layer construction of the sensor. The bare GCE electrode exhibited a semicircular arc (curve f). Compared with the bare electrode, the PEI/RuSi-MWCNTs coating exhibited increased resistance (curve a), as the MWCNTs possessed favorable conductivity and the increase in resistance was not significant. The addition of AuNPs resulted in a lower resistance of the sensor (curve b). After further modification of the electrodes by apt (curve c), BSA (curve d) and profenofos (curve e), the impedance values increased in turn. The EIS characterization and CV characterization results were consistent. The experimental results provided further evidence that the aptasensor was successfully assembled.

### 3.3. Optimization of experimental conditions

The performance of the biosensor was influenced by a variety of factors. In order to construct a sensor with optimal performance in detection, key factors such as aptamer concentration, pH of real reaction environment and incubation time of pesticide were optimized.

The pH of PBS affected the activity and stability of biomaterials, thus affecting the efficiency of sensors. Therefore, it was imperative to optimize the pH value of PBS. This was demonstrated in Fig. 4. (a), the electrochemiluminescence intensity reached its maximum at pH = 7.5 in the pH environment range of 6.0–8.5, which was due to the inhibition of the aptamer and composite activity by the pH of the solution and thus affected the affinity. Therefore, the sensor efficacy was optimal at pH 7.5.

As shown in Fig. 4. (b), ECL intensity first increased and then decreased with the increase of aptamer concentration, and the aptamer saturated at 100 nM at the electrode, and the luminescence intensity decreased when the concentration exceeded 100 nM. This was because too much aptamer accumulated on the GCE surface and therefore did not help to fixate to the GCE surface. Therefore, the optimal aptamer concentration was 100 nM.

After specific binding of profenofos to the aptamer, electron transfer was blocked and the electrochemiluminescence intensity was reduced. Therefore, incubation time was a major factor affecting sensor performance [44]. Fig. 4. (c) Showed that the optimization of the incubation time of profenofos reached its highest value at an incubation time of 40 min, which was an indication that the specific binding of the aptamer and profenofos was saturated at this time.

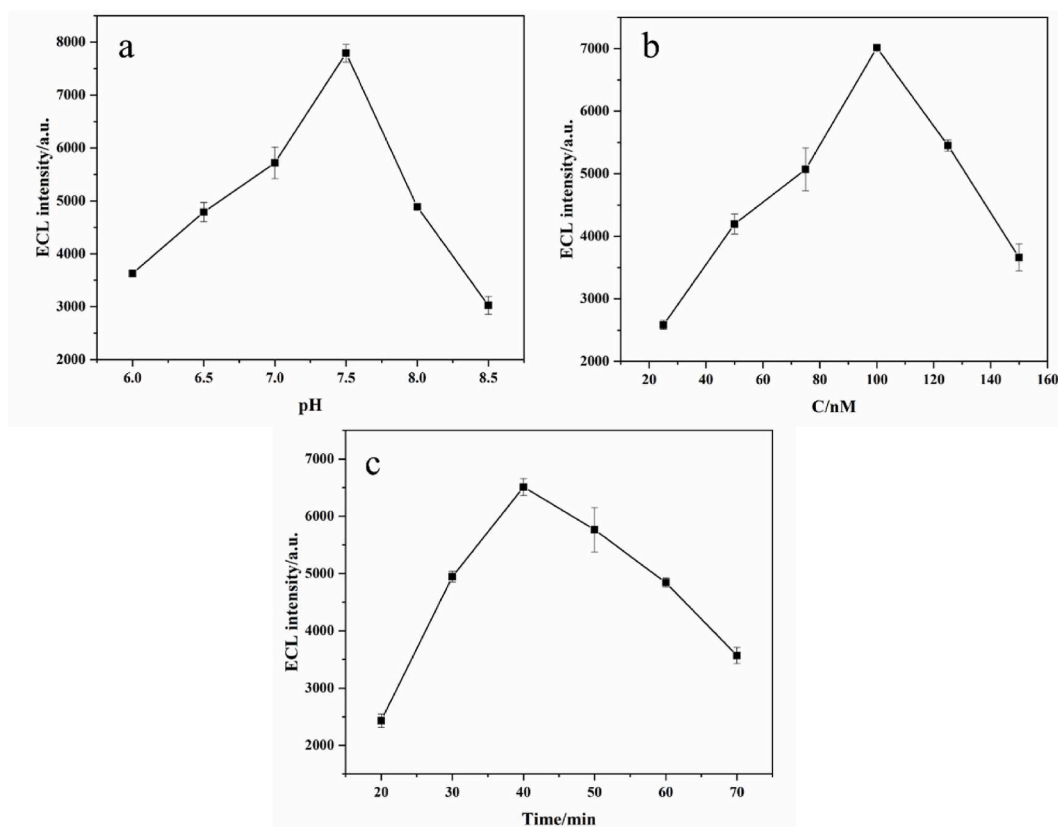


Fig. 4. Optimization of experimental parameters: (a) pH of PBS; (b) aptamer concentration; (c) incubation time.

### 3.4. Analysis of the aptasensor

Based on the experimentally optimized data, the prepared sensors were used for the detection of different concentrations of profenofos under optimal experimental conditions.

Six concentration gradients from 10 pg/mL to 1 μg/mL were set for the pesticide profenofos, as shown in Fig. 5 (A). The electrochemiluminescence intensity gradually decreased with increasing concentration of profenofos. As shown in Fig. 5 (B), the logarithm of the concentration of profenofos was inversely proportional to the electrochemiluminescence intensity, with a good linear relationship. Its linear regression equation was  $I_{ECL} = 6690.38 - 1254.63 \lg C_{\text{profenofos}} (\text{ng/mL})$ ,  $R^2 = 0.99922$ .

$$LOD = \frac{3 \times S}{K} \quad (1)$$

Here, S represented the standard deviation of the signal from the lowest detected concentration, and K denoted the slope of the aptasensor standard curve. The (LOD) was  $1.482 \times 10^{-3}$  ng/mL. The sensor's good detection performance was indicated by its lower LOD compared with other detection methods.

Table 1 listed the relevant parameters of sensors for the detection of profenofos in recent years. Compared with other sensors for detecting profenofos, this sensor was characterized by a wide linear range and low detection limit.

### 3.5. Selectivity, repeatability and stability of the aptasensor

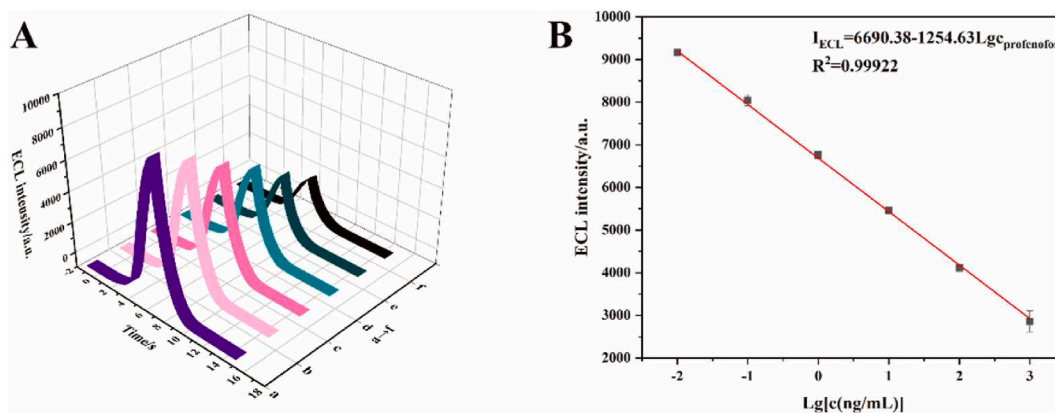
Fig. 6 (A) showed the stability test chart of the aptasensor. 15 sensors were simultaneously prepared and divided into 5 groups. A group of drops with 10 ng/mL profenofos were selected and their ECL intensities were measured under optimal experimental conditions. The remaining 4 groups of sensors were refrigerated at 4 °C, and 1 group of sensors were taken out every 7 days and tested by adding 10 ng/mL of profenofos dropwise. The ECL intensity was basically unchanged after 7th day, decreased by 2.8277 % after 14th day, and decreased by 7.3749 % after 21st day. The luminescence intensity of the sensor decreased by 10.4508 % at the 28th day. Overall, the sensor had good stability during the first 21 days and there was a significant decrease in luminescence performance at 28th day.

Fig. 6 (B) showed the repeatability test diagram of the sensor. 5 sensors were prepared simultaneously, and their ECL intensities were measured under optimal experimental conditions by the dropwise addition of 1 ng/mL profenofos. The relative standard deviation (RSD) was 1.012 % for the 5 sensors, and the results indicated that the aptasensor had fine repeatability.

We selected malathion, chlorpyrifos, acetamiprid, oxamyl and profenofos to test sensor selectivity. All concentrations of pesticides were 10 ng/mL. As shown in Fig. 6 (C), malathion, chlorpyrifos, acetamiprid, oxamyl and their mixtures did not reduce the ECL intensity of the sensor at the same concentration conditions. Both profenofos and a mixture of 5 pesticides were effective in suppressing ECL intensity. The experimental outcomes demonstrated that the sensor had remarkable specificity for profenofos.

### 3.6. Analysis of vegetable samples

In order to investigate the application of the prepared aptasensor in the detection of real samples, spinach, rape and lettuce were selected for testing. All vegetable samples were purchased from a local supermarket in Zibo, China. The vegetable samples underwent testing for the presence of profenofos using HPLC and the results were all found to be free of profenofos residues. The vegetable samples were pretreated and spiked with 1 ng/mL, 10 ng/mL and 100 ng/mL profenofos by the standard addition method to the 3 vegetable samples for extraction. Finally, the aptasensor constructed in this paper was used to perform electrochemiluminescence detection on



**Fig. 5.** (A) Electrochemiluminescence response of different concentrations of profenofos: (a)  $1 \times 10^{-2}$  ng/mL, (b)  $1 \times 10^{-1}$  ng/mL, (c)  $1 \times 10^0$  ng/mL, (d)  $1 \times 10^1$  ng/mL, (e)  $1 \times 10^2$  ng/mL, (f)  $1 \times 10^3$  ng/mL. (B) Linear relationships between ECL intensity and logarithm of profenofos concentrations.

**Table 1**  
Comparison of different sensors for the determination of Profenofos.

Method	Materials	Linear range	Detection limit	Reference
Electrochemistry	NaCl•15-crown-5/GCE	$0.383\text{--}5.74 \times 10^1$ ng/mL	$1.274 \times 10^{-1}$ ng/mL	[45]
Electrochemistry	MIP/GO/GCE	$18.68\text{--}1.3 \times 10^6$ ng/mL	$1.868 \times 10^0$ ng/mL	[46]
Fluorescence	AuNPs-cys/CDs	20–320 ng/mL	$5.5 \times 10^0$ ng/mL	[47]
ECL	BSA/Apt/ABEI-AgNPs-GO/GCE	$0.1\text{--}1 \times 10^4$ ng/mL	$6.7 \times 10^{-2}$ ng/mL	[40]
ECL	BSA/Apt/AuNPs/PEI/RuSi-MWCNTs/GCE	$0.01\text{--}1 \times 10^3$ ng/mL	$1.482 \times 10^{-3}$ ng/mL	This work

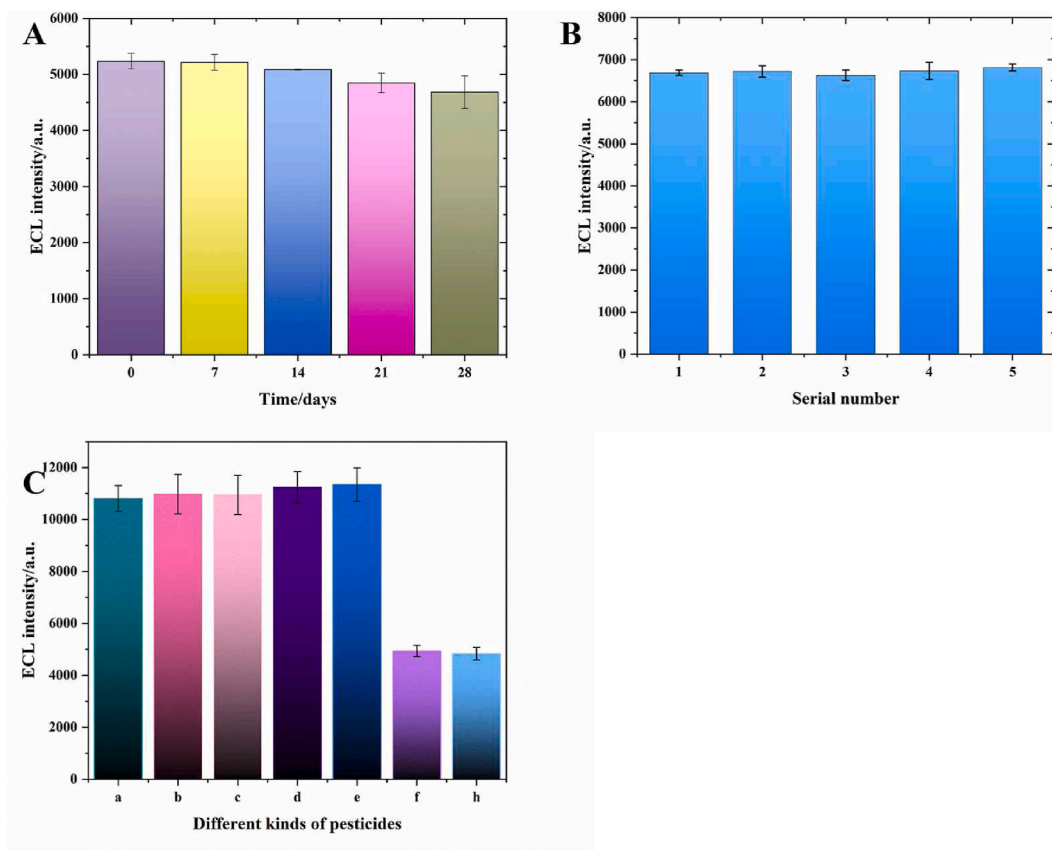


**Fig. 6.** (A) Stability of aptasensor. (B) Repeatability of aptasensor. (C) Selectivity, of aptasensor: (a) malathion; (b) chlorpyrifos; (c) acetamiprid; (d) oxamyl; (e) a mixture of the above four pesticides; (f) profenofos; (h) a mixture of the above five pesticides.

**Table 2**  
Test results of pesticide content in actual vegetable samples (n = 3).

Sample	HPLC (ng/mL)	Spiked (ng/mL)	Detected (ng/mL)	Recovery (%)	RSD (%)
Spinach	0	0	0	–	–
		1	1.0135	101.35	3.39
		10	10.387	103.87	4.85
		100	96.66	96.66	4.55
Rape	0	0	0	–	–
		1	1.0436	104.36	1.83
		10	10.043	100.43	4.45
		100	106.47	106.47	4.80
Lettuce	0	0	0	–	–
		1	0.9753	97.53	2.05
		10	10.248	102.48	4.52
		100	92.29	92.29	5.73

different concentrations of samples. The experimental results were shown in Table 2.

The results of the experiments showed that the electrochemiluminescence results for all 3 vegetable samples were close to the values for the addition of profenofos. The recoveries of the designed aptasensor ranged from 92.29 % to 106.47 %, and the RSD did not exceed 5.73 %. These findings indicated that the sensor performed well in detecting real samples.

#### 4. Conclusions

In this work, a self-enhanced electrochemiluminescent aptasensor based on the ternary nanocomposite PEI/RuSi-MWCNTs was prepared and applied for the detection of profenofos residues in vegetables. The self-enhanced complex, PEI-Ru, reduced the electron transfer distance and improved the luminescence intensity and stability. The special spatial structure and chemical bond of MWCNTs increased the solid-state loadings of RuSiNPs and PEI, which also served as a good signal amplification. The ternary composite PEI/RuSi-MWCNTs simplified the assembly process of the sensor and reduced the experimental errors. The addition of AuNPs slightly enhanced the conductivity of the sensor, and it also immobilized the aptamer by creating Au-S bonds through bonding with the sulfhydryl groups on the aptamer.

The LOD of the sensor was as low as  $1.482 \times 10^{-3}$  ng/mL with an  $R^2$  of 0.9992, and the spiked recoveries of the actual samples ranged from 92.29 % to 106.47 % with the RSDs of 1.83 %–5.73 %. In conclusion, the sensor has a low limit of detection, wide linear range, good stability, high specificity and good repeatability, which has a broad application prospect and provides an idea for the construction of ECL sensor.

#### Data availability statement

All data for this work will be made available upon request. If you require some of the data from this work, please contact the corresponding author: [fangyuan-lu@foxmail.com](mailto:fangyuan-lu@foxmail.com).

#### CRedit authorship contribution statement

**Zhenying He:** Writing – original draft, Visualization, Software, Methodology, Formal analysis, Data curation, Conceptualization. **Haifang Wang:** Software. **Wenzheng Liu:** Investigation, Data curation. **Jiashuai Sun:** Validation. **Jingcheng Huang:** Validation, Supervision. **Jie Han:** Formal analysis. **Baoxin Li:** Software. **Rui Xu:** Methodology. **Yuhao Zhang:** Visualization. **Jin Hua:** Methodology. **Yemin Guo:** Writing – review & editing, Resources, Funding acquisition, Conceptualization. **Fangyuan Lu:** Writing – review & editing, Project administration. **Ce Shi:** Validation, Funding acquisition.

#### Declaration of competing interest

The authors declare that they have no known competing financial interests or personal relationships that could have appeared to influence the work reported in this paper.

#### Acknowledgments

This work was supported by the National Natural Science Foundation of China (No.32372438, 31772068) and the Central Finance Guidance Local Science and Technology Development Fund Project (YDZX2022163), Shandong Province Major Applied Technology Innovation Project (SD2019NJ007), Technological innovation guidance project of Department of Science & Technology of Gansu Province (22CX8NA023) and Weifang Science and Technology Development Project (2021ZJ1103).

#### References

- [1] T.O. Ajiboye, P.O. Oladoye, C.A. Olanrewaju, G.O. Akinsola, Organophosphorus pesticides: impacts, detection and removal strategies, *Environ. Nanotechnol. Monit. Manag.* 17 (2022) 100655, <https://doi.org/10.1016/j.enmm.2022.100655>.
- [2] Q. Chen, Y. Sun, S. Liu, J. Zhang, C. Zhang, H. Jiang, X. Han, L. He, S. Wang, K. Zhang, Colorimetric and fluorescent sensors for detection of nerve agents and organophosphorus pesticides, *Sensor. Actuator. B Chem.* 344 (2021) 130278, <https://doi.org/10.1016/j.snb.2021.130278>.
- [3] D.-W. Jung, D.-H. Jeong, H.-S. Lee, Endocrine disrupting potential of selected azole and organophosphorus pesticide products through suppressing the dimerization of human androgen receptor in genomic pathway, *Ecotoxicol. Environ. Saf.* 247 (2022) 114246, <https://doi.org/10.1016/j.ecoenv.2022.114246>.
- [4] Y. Wu, J. Song, Q. Zhang, S. Yan, X. Sun, W. Yi, R. Pan, J. Cheng, Z. Xu, H. Su, Association between organophosphorus pesticide exposure and depression risk in adults: a cross-sectional study with NHANES data, *Environ. Pollut.* 316 (2023) 120445, <https://doi.org/10.1016/j.envpol.2022.120445>.
- [5] M. Jokanović, Neurotoxic effects of organophosphorus pesticides and possible association with neurodegenerative diseases in man: a review, *Toxicology* 410 (2018) 125–131, <https://doi.org/10.1016/j.tox.2018.09.009>.
- [6] M.E. Khalifa, I.M.M. Kenawy, Y.G. Abou El-Reash, A.B. Abdallah, Extractive separation of profenofos as an organophosphorus insecticide from wastewater and plant samples using molecular imprinted cellulose, *J. Environ. Chem. Eng.* 5 (4) (2017) 3447–3454, <https://doi.org/10.1016/j.jece.2017.07.012>.
- [7] X. Shi, H. Liu, M. Zhang, F. Yang, J. Li, Y. Guo, X. Sun, Ultrasensitive electrochemiluminescence aptasensor based on AuNPs@MWCNTs and Au@AgNPs for detection of profenofos residues, *Sensor. Actuator. B Chem.* 348 (2021) 130663, <https://doi.org/10.1016/j.snb.2021.130663>.
- [8] Y. Zhang, F.E. Deng, Determination of profenofos by high performance liquid chromatography, *Pesticides* (1996).
- [9] Y. Alen, Y. Nufika, N. Suharti, A. Djamaan, The determination of profenofos insecticide residue cabbage (*Brassica oleracea* L.) by using gas chromatography, *Der Pharma Chem.* 8 (7) (2016) 118–123.

- [10] P.G. Arias, H. Martínez-Pérez-Cejuela, A. Combès, V. Pichon, E. Pereira, J.M. Herrero-Martínez, M. Bravo, Selective solid-phase extraction of organophosphorus pesticides and their oxon-derivatives from water samples using molecularly imprinted polymer followed by high-performance liquid chromatography with UV detection, *J. Chromatogr. A* 1626 (2020) 461346, <https://doi.org/10.1016/j.chroma.2020.461346>.
- [11] Z. Ma, Y. Gao, F. Chu, Y. Tong, Y. He, Y. Li, Z. Gao, W. Chen, S. Zhang, Y. Pan, Tip-assisted ambient electric arc ionization mass spectrometry for rapid detection of trace organophosphorus pesticides in strawberry, *Chin. Chem. Lett.* 33 (9) (2022) 4411–4414, <https://doi.org/10.1016/j.ccl.2021.12.029>.
- [12] F. Zhao, J. Wu, Y. Ying, Y. She, J. Wang, J. Ping, Carbon nanomaterial-enabled pesticide biosensors: design strategy, biosensing mechanism, and practical application, *TrAC, Trends Anal. Chem.* 106 (2018) 62–83, <https://doi.org/10.1016/j.trac.2018.06.017>.
- [13] F. Zhao, Y. Yao, C. Jiang, Y. Shao, D. Barceló, Y. Ying, J. Ping, Self-reduction bimetallic nanoparticles on ultrathin MXene nanosheets as functional platform for pesticide sensing, *J. Hazard Mater.* 384 (2020) 121358, <https://doi.org/10.1016/j.jhazmat.2019.121358>.
- [14] F. Zhao, J. He, X. Li, Y. Bai, Y. Ying, J. Ping, Smart plant-wearable biosensor for in-situ pesticide analysis, *Biosens. Bioelectron.* 170 (2020) 112636, <https://doi.org/10.1016/j.bios.2020.112636>.
- [15] K. Brown, R.S. Blake, L. Dennany, Electrochemiluminescence within veterinary Science: a review, *Bioelectrochemistry* 146 (2022) 108156, <https://doi.org/10.1016/j.bioelechem.2022.108156>.
- [16] Y. Zhao, Y. Zhang, G. Jie, An “on-off” electrochemiluminescence biosensor based on DNA nanotweezer probe coupled with tripod capture DNA for high sensitive detection of Pb<sup>2+</sup>, *Sensor. Actuator. B Chem.* 326 (2021) 128985 <https://doi.org/10.1016/j.snb.2020.128985>.
- [17] F. Zhao, L. Wang, M. Li, M. Wang, G. Liu, J. Ping, Nanozyme-based biosensor for organophosphorus pesticide monitoring: functional design, biosensing strategy, and detection application, *TrAC, Trends Anal. Chem.* 165 (2023) 117152, <https://doi.org/10.1016/j.trac.2023.117152>.
- [18] F. Yue, H. Li, Q. Kong, J. Liu, G. Wang, F. Li, Q. Yang, W. Chen, Y. Guo, X. Sun, Selection of broad-spectrum aptamer and its application in fabrication of aptasensor for detection of aminoglycoside antibiotics residues in milk, *Sensor. Actuator. B Chem.* 351 (2022) 130959, <https://doi.org/10.1016/j.snb.2021.130959>.
- [19] V.G. Amelin, D.S. Bol'Shakov, A.M. Andorlov, Screening and determination of pesticides from various classes in natural water without sample preparation by ultra HPLC–high-resolution quadrupole time-of-flight mass spectrometry, *J. Anal. Chem.* 73 (3) (2018) 257–265, <https://doi.org/10.1134/S1061934818030024>.
- [20] A. Mj, C.A. Chen, A. Jh, B. Hz, A. Zx, Fluorescence assay for three organophosphorus pesticides in agricultural products based on Magnetic-Assisted fluorescence labeling aptamer probe, *Food Chem.* 307 (2020) 125534, <https://doi.org/10.1016/j.foodchem.2019.125534>.
- [21] S.I. Hori, A. Herrera, J.J. Rossi, J. Zhou, Current advances in aptamers for cancer diagnosis and therapy, *Cancers* 10 (1) (2018) 9.
- [22] M. Liu, A. Khan, Z. Wang, Y. Liu, G. Yang, Y. Deng, N. He, Aptasensors for pesticide detection, *Biosens. Bioelectron.* 130 (2019) 174–184, <https://doi.org/10.1016/j.bios.2019.01.006>.
- [23] Y. Kim, J. Kim, Modification of indium tin oxide with dendrimer-encapsulated nanoparticles to provide enhanced stable electrochemiluminescence of Ru(bpy)<sub>3</sub><sup>3+</sup>/tripropylamine while preserving optical transparency of indium tin oxide for sensitive electrochemiluminescence-based analyses, *Anal. Chem.* 86 (3) (2014) 1654–1660, <https://doi.org/10.1021/ac403415m>.
- [24] Z. Zhang, H. Yu, Y. Zhang, Z. Wang, H. Gao, S. Rong, L. Meng, J. Dai, H. Pan, D. Chang, A sandwich-configuration electrochemiluminescence immunoassay based on Cu<sub>2</sub>O@OMC-Ru nanocrystals and OMC-MoS<sub>2</sub> nanocomposites for determination of alpha-fetoprotein, *Microchim. Acta* 188 (6) (2021) 213, <https://doi.org/10.1007/s00604-021-04848-4>.
- [25] M. Li, H. Yang, C. Ma, Y. Zhang, S. Ge, J. Yu, M. Yan, A sensitive signal-off aptasensor for adenosine triphosphate based on the quenching of Ru(bpy)<sub>3</sub><sup>3+</sup>-doped silica nanoparticles electrochemiluminescence by ferrocene, *Sensor. Actuator. B Chem.* 191 (2014) 377–383, <https://doi.org/10.1016/j.snb.2013.10.020>.
- [26] J. Ma, L. Wu, Z. Li, Z. Lu, W. Yin, A. Nie, F. Ding, B. Wang, H. Han, Versatile electrochemiluminescence assays for PEDV antibody based on rolling circle amplification and Ru-DNA nanotags, *Anal. Chem.* 90 (12) (2018) 7415–7421, <https://doi.org/10.1021/acs.analchem.8b00853>.
- [27] H. Wang, Y. He, Y. Chai, R. Yuan, A super intramolecular self-enhanced electrochemiluminescence immunosensor based on polymer chains grafted on palladium nanocages, *Nanoscale* 6 (17) (2014) 10316–10322, <https://doi.org/10.1039/c4nr02808b>.
- [28] N. Cao, F. Zhao, B. Zeng, A novel self-enhanced electrochemiluminescence sensor based on PEI-CdS/Au@SiO<sub>2</sub>@RuDs and molecularly imprinted polymer for the highly sensitive detection of creatinine, *Sensor. Actuator. B Chem.* 306 (2020) 127591, <https://doi.org/10.1016/j.snb.2019.127591>.
- [29] Y. Yuan, L. Zhang, H. Wang, Y. Chai, R. Yuan, Self-enhanced PEI-Ru(II) complex with polyamino acid as booster to construct ultrasensitive electrochemiluminescence immunosensor for carcinoembryonic antigen detection, *Anal. Chim. Acta* 1001 (2018) 112–118, <https://doi.org/10.1016/j.aca.2017.11.035>.
- [30] S. Iijima, Helical microtubules of graphitic carbon, *Nature* 354 (6348) (1991) 56–58.
- [31] L. Ma, L. Bai, M. Zhao, J. Zhou, Y. Chen, Z. Mu, An electrochemical aptasensor for highly sensitive detection of zearalenone based on PEI-MoS<sub>2</sub>-MWCNTs nanocomposite for signal enhancement, *Anal. Chim. Acta* 1060 (2019) 71–78, <https://doi.org/10.1016/j.aca.2019.02.012>.
- [32] Y. Su, Y. Liang, H. Wu, J. Jiang, W. Lai, C. Zhang, A three-dimensional cloth-based microfluidic label-free proximity hybridization-electrochemiluminescence biosensor for ultrasensitive detection of K-ras gene, *Sensor. Actuator. B Chem.* 296 (2019) 126654, <https://doi.org/10.1016/j.snb.2019.126654>.
- [33] G.C. Nayak, R. Rajasekar, C.K. Das, Dispersion of SiC coated MWCNTs in PEI/silicone rubber blend and its effect on the thermal and mechanical properties, *J. Appl. Polym. Sci.* 119 (6) (2010) 3574–3581, <https://doi.org/10.1002/app.33021>.
- [34] R. Singh, S. Kumar, F.Z. Liu, C. Shuang, B.K. Kaushik, Etched multicore fiber sensor using copper oxide and gold nanoparticles decorated graphene oxide structure for cancer cells detection, *Biosens. Bioelectron.* 168 (6) (2020) 112557, <https://doi.org/10.1016/j.bios.2020.112557>.
- [35] G. Mo, X. He, C. Zhou, D. Ya, J. Feng, C. Yu, B. Deng, A novel ECL sensor based on a boronate affinity molecular imprinting technique and functionalized SiO<sub>2</sub>@CQDs/AuNPs/MPBA nanocomposites for sensitive determination of alpha-fetoprotein, *Biosens. Bioelectron.* 126 (2019) 558–564, <https://doi.org/10.1016/j.bios.2018.11.013>.
- [36] F. Zhao, Y. Yao, X. Li, L. Lan, C. Jiang, J. Ping, Metallic transition metal dichalcogenide nanosheets as an effective and biocompatible transducer for electrochemical detection of pesticide, *Anal. Chem.* 90 (19) (2018) 11658–11664, <https://doi.org/10.1021/acs.analchem.8b03250>.
- [37] Y. Zhuo, N. Liao, Y.-Q. Chai, G.-F. Gui, M. Zhao, J. Han, Y. Xiang, R. Yuan, Ultrasensitive apurinic/apryrimidinic endonuclease 1 immunosensing based on self-enhanced electrochemiluminescence of a Ru(II) complex, *Anal. Chem.* 86 (2) (2014) 1053–1060, <https://doi.org/10.1021/ac403019e>.
- [38] C. Miao, A. Zhang, Y. Xu, C. Shen, F. Ma, C. Huang, N. Jia, An ultrasensitive electrochemiluminescence sensor for detecting diphenhydramine hydrochloride based on l-cysteine-functionalized multiwalled carbon nanotubes/gold nanoparticles nanocomposites, *Sensor. Actuator. B Chem.* 213 (2015) 5–11, <https://doi.org/10.1016/j.snb.2015.02.069>.
- [39] Y. Yuan, Z. Ling, H. Wang, Y. Chai, R. Yuan, Self-enhanced PEI-Ru(II) complex with polyamino acid as booster to construct ultrasensitive electrochemiluminescence immunosensor for carcinoembryonic antigen detection, *Anal. Chim. Acta* 1001 (2018) 112–118, <https://doi.org/10.1016/j.aca.2017.11.035>.
- [40] J. Han, Y. Yu, G. Wang, X. Gao, L. Geng, J. Sun, M. Zhang, X. Meng, F. Li, C. Shi, X. Sun, Y. Guo, M.B.M. Ahmed, Ultrasensitive electrochemiluminescence aptasensor based on ABEI reduced silver nanoparticles for the detection of profenofos, *Sci. Total Environ.* 844 (2022) 157184, <https://doi.org/10.1016/j.scitotenv.2022.157184>.
- [41] M.-S. Wu, L.-J. He, J.-J. Xu, H.-Y. Chen, RuSi@Ru(bpy)<sub>3</sub><sup>3+</sup>/Au@Ag<sub>2</sub>S nanoparticles electrochemiluminescence resonance energy transfer system for sensitive DNA detection, *Anal. Chem.* 86 (9) (2014) 4559–4565, <https://doi.org/10.1021/ac500591n>.
- [42] W. Yan, L. Xu, C. Xu, W. Ma, H. Kuang, L. Wang, N.A. Kotov, Self-assembly of chiral nanoparticle pyramids with Strong R/S optical activity, *J. Am. Chem. Soc.* 134 (36) (2012) 15114–15121, <https://doi.org/10.1021/ja3066336>.
- [43] L.-R. Hong, Y.-Q. Chai, M. Zhao, N. Liao, R. Yuan, Y. Zhuo, Highly efficient electrogenerated chemiluminescence quenching of PEI enhanced Ru(bpy)<sub>3</sub><sup>3+</sup> nanocomposite by hemin and Au/CeO<sub>2</sub> nanoparticles, *Biosens. Bioelectron.* 63 (2015) 392–398, <https://doi.org/10.1016/j.bios.2014.07.065>.
- [44] X. Shi, F. Yang, H. Liu, M. Zhang, Y. Guo, Supersensitive electrochemiluminescence aptasensor for malathion residues based on ATO@TiO<sub>2</sub> and AgNPs, *Food Anal. Methods* 13 (2021), <https://doi.org/10.1007/s12161-021-02066-5>.

- [45] N. Nesakumar, I. Suresh, G.B. Jegadeesan, J.B.B. Rayappan, A.J. Kulandaiswamy, An efficient electrochemical sensing platform for profenofos detection, *Measurement* 202 (2022) 111807, <https://doi.org/10.1016/j.measurement.2022.111807>.
- [46] M.E. Khalifa, A.B. Abdallah, Molecular imprinted polymer based sensor for recognition and determination of profenofos organophosphorous insecticide, *Biosens. Bioelectron. X* 2 (2019) 100027, <https://doi.org/10.1016/j.biosx.2019.100027>.
- [47] F. Liu, S. Zhao, X. Lai, Y. Fan, P. Han, L. Chen, Colorimetric and fluorescent probes for the rapid detection of profenofos in farmland system, *Food Chem.* 393 (2022) 133321, <https://doi.org/10.1016/j.foodchem.2022.133321>.